

Analysis of Microwave and Hard X-ray Emissions in Solar Eruptive Events

Yu-Lun Liou (劉宇倫)

Department of Atmospheric Sciences, National Central University (中央大學大氣系)

Supervisor: Prof. Ya-Hui Yang (楊雅惠)

Graduate Institute of Space Science, National Central University (中央大學太空所)

ABSTRACT

In this summer program, we used the observational data from the *Nobeyama Radioheiligograph* (NoRH) and the *Reuven Ramaty High-Energy Solar Spectroscopic Imager* (RHESSI) to investigate a limb solar flare event on 2012 July 19. This flare shows a clear loop structure in the radio images together with the loop-top and footpoint sources in the hard X-ray (HXR) images. Moreover, the strong radio and HXR sources are found to locate at different footpoints of the flaring loop. By combining with theories, we speculate that the southern footpoint should have the stronger magnetic field than the northern one.

INTRODUCTION

Solar flare is one of the most explosive phenomena in solar system, characterized by the sudden brightening seen in solar images with various shapes. It is believed that the energy stored in the complex magnetic fields could be released via the magnetic reconnection process in the corona and then converted to the charged particles' thermal and kinetic energies. The electrons can be accelerated up to several MeV. When these accelerated electrons move along the magnetic fields down to the chromospheres and collide with other ions, the precipitated and trapped electrons would produce hard X-ray (HXR) and radio emissions by different mechanisms.

In general, the time profiles of HXR and radio emissions in solar flares are similar because they are mostly come from the same population of non-thermal electrons. However, their emission mechanisms are quite different. The bremsstrahlung (also called free-free) emission is dominant in HXR, while the gyrosynchrotron emission is dominant in microwaves.

In the fully ionized plasma, the free electron collides with free ion resulting in radiations, as illustrated in Figure 1. Such bremsstrahlung emission can be further divided into two types, i.e., *Thin-target* and *Thick-target* bremsstrahlung, depending on the density of target ions. As shown in Figure 2, if the accelerated electrons impact sparse ions, the low-energy HXR emission would be produced due to the thin-target bremsstrahlung. However, when the accelerated electrons precipitate into dense ions, it

would emit high-energy HXR due to thick-target bremsstrahlung. On the other hand, gyrosynchrotron emissions are generated by the electrons which undergo gyro-motion trapped by the magnetic fields due to Lorentz force, as shown in Figure 3. Therefore, the stronger radio emissions would be expected to appear at the stronger magnetic field regions. Readers are referred to Aschwanden (1996) for more detailed discussions about emission mechanisms.

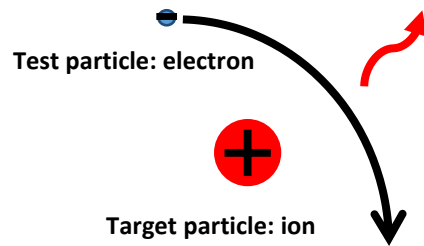


Figure 1. Illustration of bremsstrahlung emission.



Figure 2. Illustration of thin-target (left) and thick-target (right) bremsstrahlung.

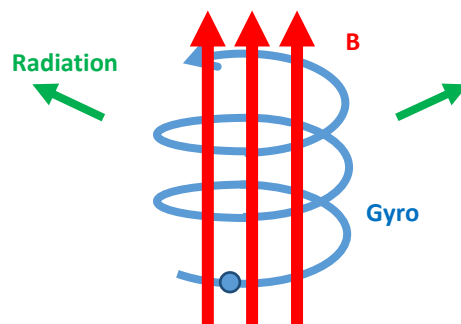


Figure 3. Illustration of gyrosynchrotron emission.

According to a flare standard model illustrated in Figure 4, the accelerated electrons escaped from the reconnection would emit microwave and low-energy HXR emissions in the corona. When these accelerated electrons move down to the dense chromospheres, the precipitated electrons would emit high-energy HXR emission and the trapped

electrons would produce radio emission. Combining the spectral (Ning 2007; Kawate et al. 2012; Asai et al. 2013) and imaging analyses would be useful for understanding the particle acceleration mechanism in solar flares. But we only focus on the imaging analysis in this report.

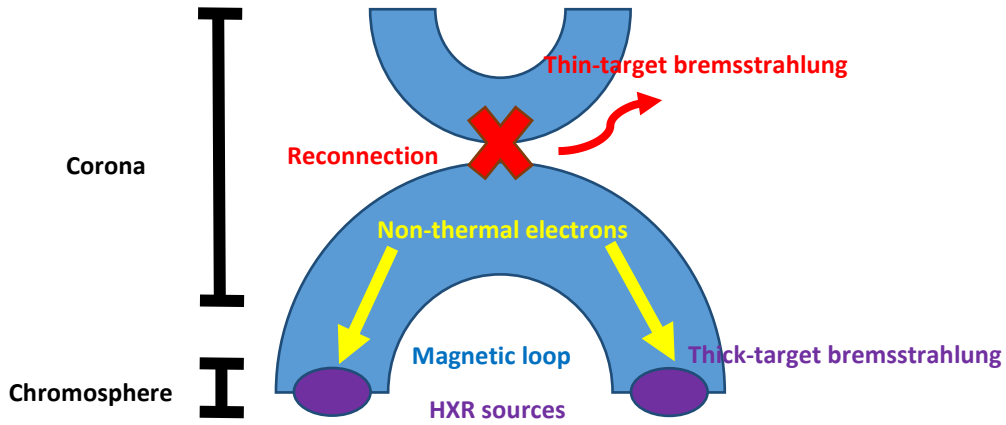


Figure 4. Illustration of particle accelerations in a solar flare.

OBSERVATIONAL DATA

The HXR data used in this summer program is obtained from *Reuven Ramaty High-Energy Solar Spectroscopic Imager* (RHESSI; Lin et al. 2002) spacecraft. RHESSI provides a wide band measurement from X-ray to γ -ray with the high angular resolution (logarithmically from 2.3'' to 180'') and the high spectral resolution (1 keV in the X-ray range). We used the CLEAN algorithm (Hurford et al. 2002) to reconstruct HXR images. On the other hand, the radio data used here is obtained from *Nobeyama Radioheiligograph* (NoRH; Nakajima et al. 1991). NoRH is a radio telescope dedicated to observe the sun. It consists of 84 antennas with 80 cm diameter and provides 17 GHz and 34 GHz observations with the angular resolution of 14 and 7 arcseconds separately. All data are analyzed using IDL-based software (called *SolarSoftware*).

We selected the M7.7 flare event on 2012 July 19 for study, which occurred near the solar west limb with well coverage of RHESSI and NoRH data in the impulsive phase. The basic information of the studied event is list in Table 1.

Table 1. Basic information of studied event

| Date | Class | Start time | Peak time | End time | Location |
|-------------|-------|------------|-----------|----------|----------|
| 2012 Jul 19 | M7.7 | 04:58:16 | 05:27:30 | 05:33:28 | S14 W79 |

RESULTS

Figure 5 shows the lightcurves of HXR emissions in the range of 25-50 keV (purple) and radio emissions in the 17 GHz (origin). Both HXR and radio emissions generally have similar temporal variations. To reconstruct HXR images, we selected two time intervals covering the main and subsequent peaks for imaging analysis, as denoted by the int.1 and int.2 in the plot. Figure 6 shows the RHESSI CLEAN maps derived from different energy bands in the intervals 1 (top panel) and 2 (bottom panel). It is obvious that the HXR emissions in the low and high energy bands reveal different structures, which represents the different HXR sources produced by different mechanisms. The loop-top source is clearly seen in the low energy band but the footpoint sources become dominated in the high energy bands. Moreover, note that these conjugate footpoints have different HXR emissions, i.e., the northern HXR footpoint is stronger than the southern one. Such feature of asymmetric HXR footpoint sources is commonly seen in solar flares and can be explained by the asymmetric magnetic mirror motion at two conjugate footpoints (e.g., Yang et al. 2012).

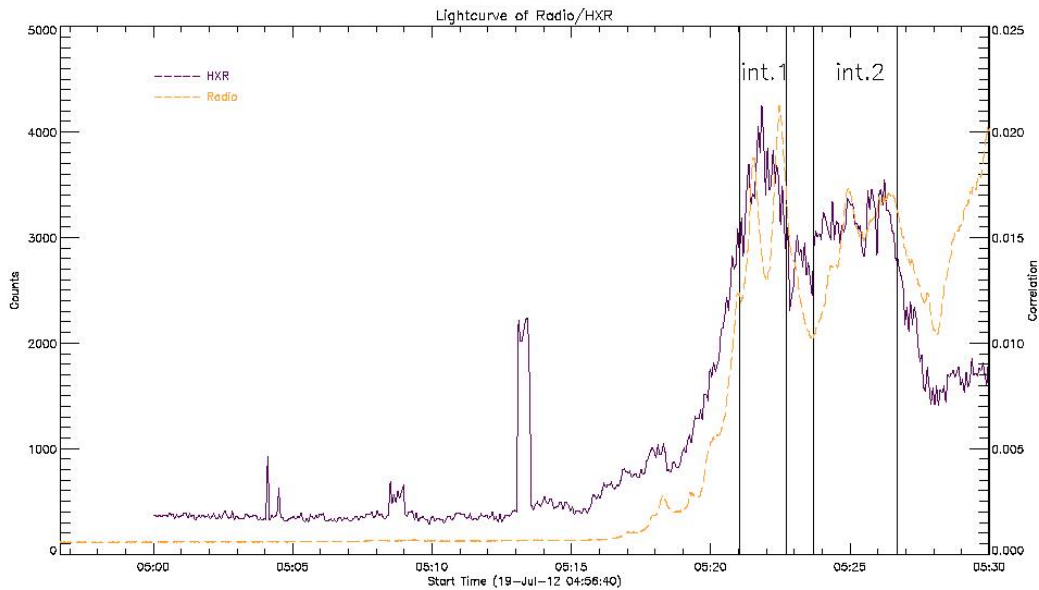


Figure 5. Lightcurves of HXR 25-50 keV (purple) and radio 17 GHz (orange) emissions, where the int.1 and int.2 denote the time intervals for HXR analysis.

Similarly, Figure 7 shows the HXR and radio lightcurves in the 25-50 keV (red) and 17 GHz (blue), but now four time intervals (vertical lines) are selected for radio analysis. Figure 8 shows the NoRH 17 GHz images at the four sub-peak times. The flare-related radio emissions appear as an arched structure rather than kernels. Moreover, the strong radio sources seem to move upward along the magnetic loop as the flare proceeds.

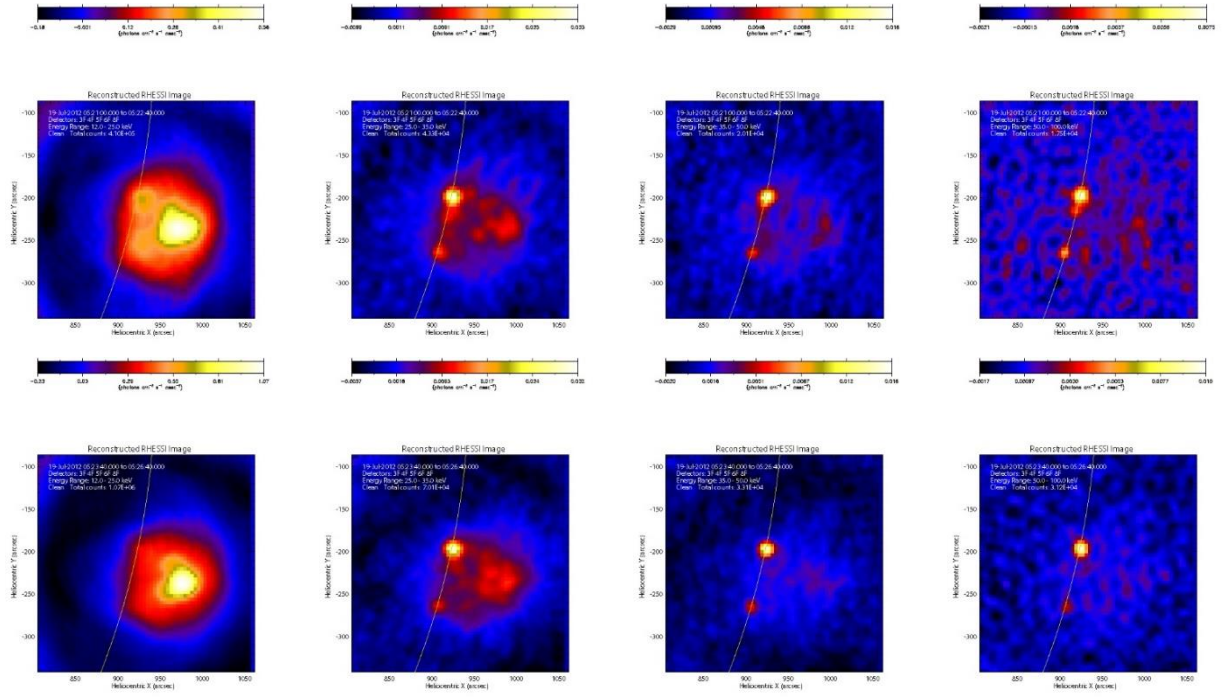


Figure 6. RHESSI CLEAN maps for different energy bands in intervals 1 (top) and 2 (bottom).

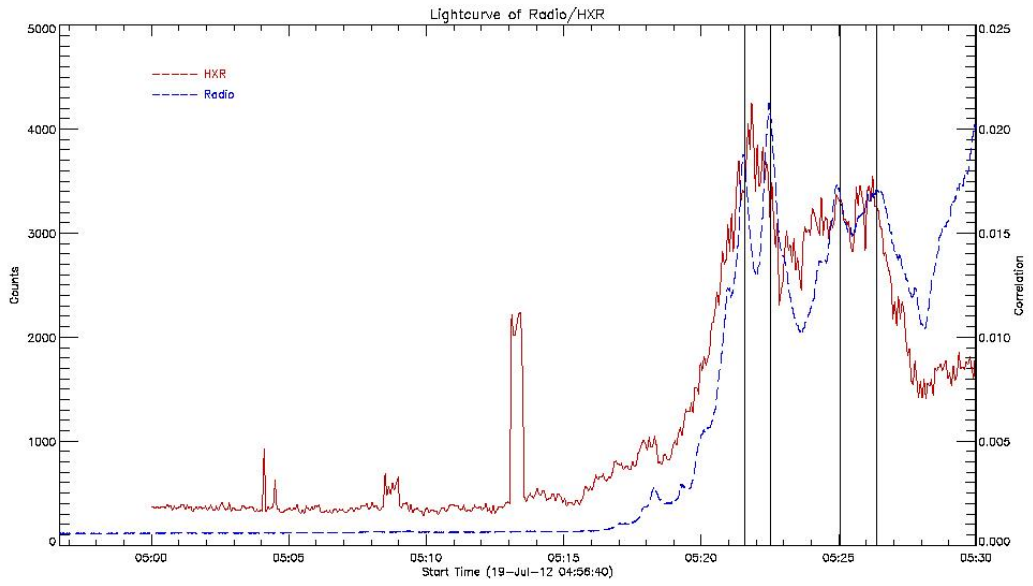


Figure 7. Lightcurves of HXR 25-50 keV (red) and radio 17 GHz (blue) emissions, where the vertical lines denote the time intervals for radio analysis.

By comparing the radio 17 GHz emissions (white contour) with the HXR 50-100 keV sources (background image) in Figure 9, we found that the stronger radio source locates at the southern footpoint, which is different from the HXR observations. Since

the radio emission is associated with the trapped electrons in the magnetic fields, such feature could imply that the magnetic field is stronger in the southern footpoint of flaring loop.

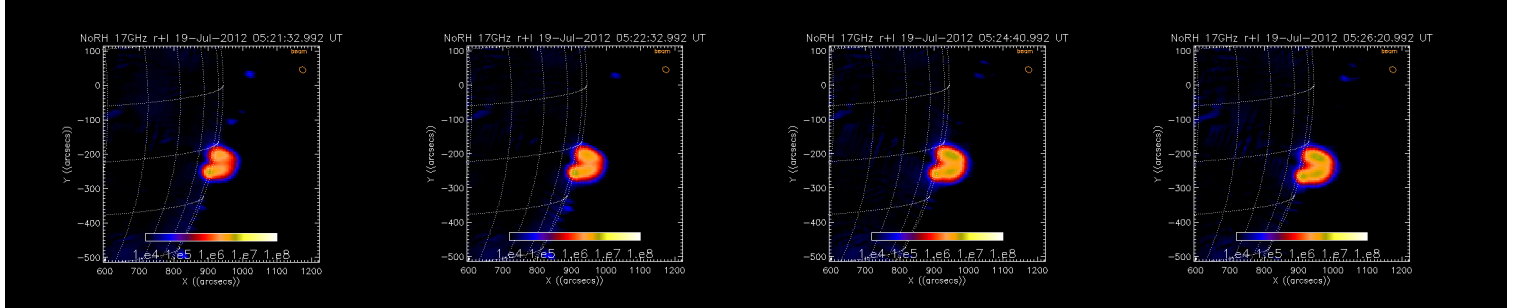


Figure 8. Radio 17 GHz images at four sub-peak times.

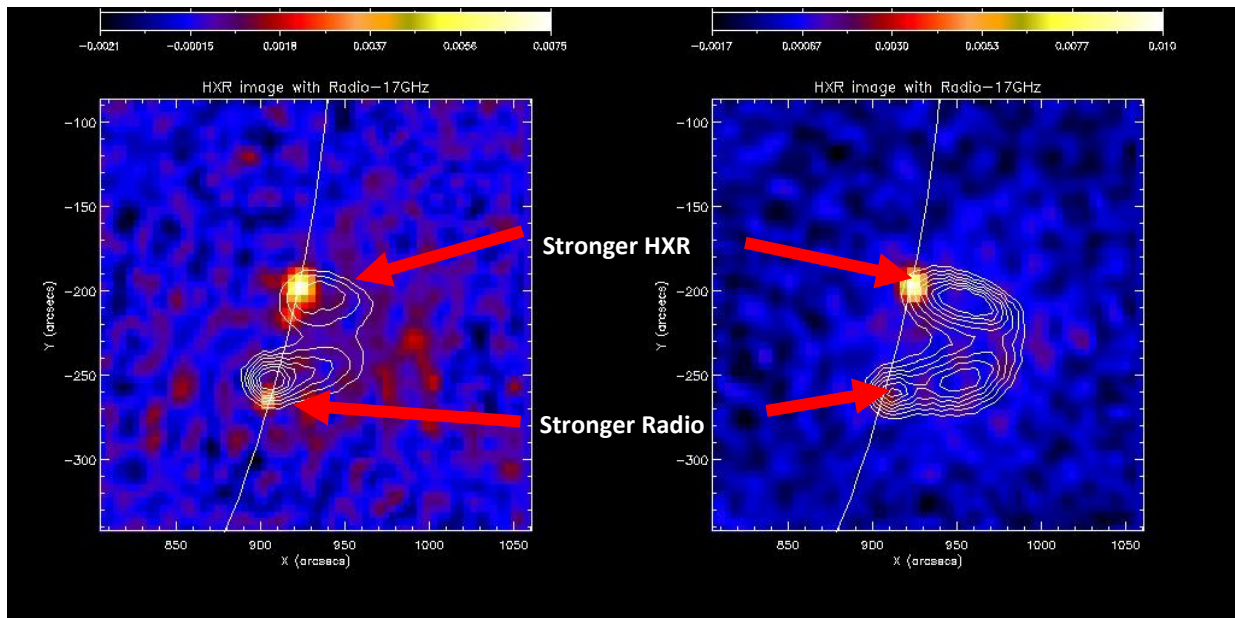


Figure 9. Comparison of HXR 50-100 keV sources (background image) and radio 17 GHz emissions (white contour).

SUMMARY

In this program, we investigated the M7.7 flare on 2012 July 19 by analyzing the RHESSI and NoRH imaging data in the impulsive phase. By combining the observations with theories, we recognized that the HXR footpoint source would be produced by the thick-target bremsstrahlung, the HXR loop-top source would be due to the thin-target bremsstrahlung, and the radio loop-like source would be generated by the gyrosynchrotron emission. Besides, we found that the strong radio source is located at

the southern footpoints of the flaring loop, which is different from the strong HXR source at the northern footpoint. Based on the gyro-motion and mirror motion of trapped particles, we speculate that the southern footpoint should have the stronger magnetic field than the northern one.

REFERENCES

- Asai, A., Kiyohara, J., Takasaki, H., Narukage, N., Yokoyama, T., Masuda, S., Shimojo, M. & Nakajima, H., 2013, *ApJ*, 763, 87
- Aschwanden, M., 2006, *Physics of the solar corona: an introduction with problems and solutions*
- Hurford, G. J., et al. 2002, *Sol. Phys.*, 210, 61
- Kawate, T., Nishizuka, N., Oi, A., Ohya, M., & Nakajima, H., 2012, *ApJ*, 747, 131
- Lin, R. P., et al. 2002, *Sol. Phys.*, 210, 3
- Nakajima, H., et al. 1991, *A New Radioheliograph at Nobeyama (Nobeyama Radio Obs. Tech. Rep. 28)*
- Ning, Z., 2007, *ApJ*, 659, L69
- Yang, Y.-H., Cheng, C. Z., Krucker, S., Hsieh, M.-S., & Chen, N.-H., 2012, *ApJ*, 756, 42